J Am Oil Chem Soc (2008) 85:405–412
DOI 10.1007/s11746-008-1227-9

ORIGINAL PAPER

In Situ Rheo-NMR Measurements of Solid Fat Content

Gianfranco Mazzanti · Elizabeth M. Mudge ·
Emmanuel Y. Anom

Received: 5 October 2007 / Revised: 14 January 2008 / Accepted: 27 February 2008 / Published online: 15 March 2008

Abstract The properties of crystallized fats depend on their solid fat content (SFC) and their fractal structures. The SFC and the structures are dramatically affected during crystallization under shear flow. A mini-Couette cell was developed to crystallize fat samples under shear. The cell was tested with blends of canola stearin (CS) in canola oil (CO) in a 20-MHz NMR spectrometer. The blends were placed in the cell, melted at 80 °C, and then crystallized under different shear rates (58–460 s^{-1}) at 40 °C inside the spectrometer for 4 h. Time averaged NMR free induction decay (FID) curves were captured at 20 s intervals. SFC values were calculated using parameters determined by a calibration procedure. The SFC values determined by the direct method with and without the shaft of the Couette device were reasonably close. Similar results were observed with and without shear in the Couette device. The FID curves did not show a significant difference either. Therefore this system is accurate for in-situ time-resolved determination of SFC under shear flow. Furthermore, a combination of the direct and the indirect methods was successfully used to estimate the temperature increase due to viscous heating. The system developed will help in understanding the effects of shear flow on SFC of nano-structured lipid multicomponent systems. This will permit the optimization of the manufacturing processes.

Keywords Fat crystallization · Polymorphism · Rheology

G. Mazzanti (✉) · E. M. Mudge · E. Y. Anom
Department of Process Engineering and Applied Science,
Dalhousie University, D405-1360 Barrington st,
B3J 2X4 Halifax, NS, Canada
e-mail: Gianfranco.Mazzanti@dal.ca

Introduction

The manufacture of lipid systems such as bakery or confectionery fats and cosmetic products relies on the formation of adequate crystalline structures. These structures range from the nanostructures of the crystalline molecular architecture to the fractal microstructures made by clusters of crystallites [1]. An essential physical characteristic of these fractal structures is the volume fraction of solids, directly related to the solid fat content (SFC). A good product requires adequate formulation, together with an appropriate balance of SFC, polymorphic form and microcrystalline structure. This balance is usually accomplished by a combination of shear flow and temperature profiles during crystallization. The mechanical, sensorial, thermal and diffusional properties of the product are thus tailored to the consumers needs.

Since its introduction, pulsed nuclear magnetic resonance (pNMR) has proven to be an invaluable tool for the determination of SFC. pNMR is the only non-destructive direct method available at present for such measurement [2–6]. However, commercial NMR systems used to determine SFC do not provide the possibility of studying the kinetics of crystallization under controlled shear flow. This measurement would be useful because shear has enormous impact on crystallization kinetics [7–10], and it is used industrially everywhere. This equipment is called a rheo-NMR system [11], because it allows the measurement of NMR properties under flowing conditions to be carried out. The SFC has been previously determined in-situ under mixing conditions (stirred tank) using a unilateral magnet system. However, in that study, the crystallizing material was subject to a large array of non-controlled shear rate values that are essentially impossible to determine [4]. In contrast, our flow system approximates a Couette flow condition. This offers a controlled way of studying the effects of shear flow, since the flow pattern is clearly defined.

When shear flow is applied to crystallizing lipid systems, it increases the speed of crystallization, reduces the transition time of different polymorphic forms [7] and alters the phase composition of the final product. It is theoretically possible to discriminate the SFC between polymorphic phases [12] by NMR, though this is not easily done. However, by applying shear flow to a sample as it crystallizes inside an NMR system, manufacturers can obtain valuable information. This information can be used to develop consistent products. For instance, creating conditions within the pNMR similar to processing conditions they can obtain better estimates of SFC compared to standard static measurements. Static measurements, such as the AOCS methods, require tempering conditions that may not be representative of their actual process.

The SFC can be determined by two different methods, direct and indirect [13]. The indirect method requires only the liquid signal of the proton relaxation. However, the indirect method requires more than one measurement, because one must compare the measurements to the pure liquid signal at the same temperature, or to a standard at two temperatures. The direct method requires a simultaneous determination of both the solid and liquid signals. The ratio of the two signals gives the SFC.

In this paper we present a device that allows one to carry out the determination of SFC under controlled shear flow, which had not been accomplished before. Both the direct and indirect methods are evaluated, which allows us to discuss the possibilities and limitations offered by this apparatus. The combined use of both methods offers a way to estimate the viscous heating of the sample, a critical parameter in crystallization under shear.

Materials and Methods

Equipment

Our shearing device consists of a motor with a speed sensor used to provide feed-back control, a frame to hold the motor on the Minispec, a holder for the 10-mm NMR tube and a special shear shaft. The shaft must be made of a material that does not interfere with the NMR measurements, thus we chose to use a Teflon® shaft attached to the motor. The shaft can be introduced to the bottom of a standard 10-mm NMR tube and used to stir the sample, thus creating a mini Couette cell in the bottom part of the tube. The upper part of the shaft has very little clearance to the inner diameter of the tube to prevent the shaft from wobbling. The bottom part, which is where the sample is located, is about 6 mm in diameter, allowing for a gap of approximately 1.5 mm since the inner glass tube diameter is ca. 9 mm. The shear rate $\dot{\gamma}$ can be estimated to first order from the relationship

$$\dot{\gamma} = \frac{u}{\delta} = \frac{2\pi\dot{\omega}r}{\delta} \qquad (1)$$

where u is the tangential velocity of the shaft, δ is the gap, $\dot{\omega}$ is the angular velocity of the shaft (rad/s), and r is the radius of the shaft. With these small radii, the curvature may induce a deviation from the ideal Couette flow, which can be calculated if necessary. For the purposes of this proof of concept we will use the nominal shear rate calculated with the above equation.

The NMR instrument in our lab is an old model of a Bruker Minispec PC20. The free induction decay (FID) signal from the Minispec for the direct method was acquired by a computer using LabView® with a 20-MHz board (ADLink-PCI9810) from the analog output of the instrument. For the indirect method, a 48-kHz board (National Instruments) was used. Ten NMR FID curves were captured with a recycle time of 2 s to produce a time averaged signal at 20 s intervals, and the SFC values were calculated using parameters determined by a calibration procedure as explained later on.

The magnet inside the NMR is kept by a thermostat at a fixed temperature near 40 °C, and our older model did not have the option of other temperatures, therefore the test material chosen was a high melting point material. We chose to use fully hydrogenated canola oil, hereafter called canola stearin (CS), and commercial canola oil (CO) mixtures to illustrate the use of the shear shaft.

Results and Discussion

Verification of SFC Determination with the Shear Shaft

Mixtures of 10, 20 and 40% CS in CO were prepared, melted at 80 °C in a water bath and placed in standard 10-mm NMR tubes. They were then equilibrated at 40 °C in a water bath for several hours, placed in the NMR and the SFC was measured directly using 10 averaged signals per reading, taking 10 readings, from the display output of the Minispec. Similar treatment was done to the mixtures placed in the tube that contained the Teflon shaft. The reduction in volume of the sample compared to a regular 10-mm glass tube without the shaft is about 40%. The measured results showed little to no significant difference in the average SFC (less than 1.5%), though there was a slightly higher variance between the samples in the tubes with the shaft versus without the shaft. This higher variance is most likely due to a lower signal to noise ratio that can be attributed to the smaller sample size.

FID signals were captured for a mixture of 20% CS in CO equilibrated at 40 °C. The FID curves are presented in Fig. 1. It was possible to obtain an almost perfect super imposed FID curve with the shaft (that produced less signal intensity) over the curve without the shaft simply by multiplying all values by 1.072. There is a slight change in the characteristic transversal decay time of the liquid signal T_2*, but it does not significantly affect the first 100 µs where the signal for the direct calculation of SFC is taken.

Care should be taken to fill the tube with enough sample so that the material completely covers the volume that can be sensed by the radio frequency coil (RFC). However, during crystallization of high SFC blends a reduction of the liquid signal was observed together with a reduction of the SFC. This could be caused by an increase in temperature, which produces a lower voltage output signal or by a contraction of the fat sample, which causes a reduction in volume. The first case can be ruled out since we tested the NMR with a sample of liquid oil for four hours and did not observe any drift in the liquid signal. The latter thus seems to be the explanation and therefore it calls for a slightly larger sample size than the one we actually used in our experiments to ensure that possible contraction will not result in a lower level of sample. The increase in sample density, however, will slightly increase the spatial density of protons within the sensing volume of the RFC, and this may result in an overall higher signal. This should not affect significantly the SFC ratio using the direct method, but will affect measurements of the liquid used commonly in the indirect SFC determination.

After equilibrating a 40% CS in CO sample under shear flow (230 s^{-1}) for 4 h, the shear was turned on and off alternatively for periods of 10 min to observe if there was an effect of shear on the FID signal. Four FID curves with shear and four FID curves without shear are plotted together in Fig. 2. It can be seen that there is no significant difference between the data sets, thus applying shear has no effect on the output signal and SFC.

Calibration of FID Signals

Bruker calibration standards were used to determine the correction factors needed for the calculation of the SFC ratio. The values used were different from those that the electronics of the NMR obtains automatically, because our sampling times in the free induction decay curve were slightly different. The difference in the sampling times was necessary because the electronic sampling of the signal in the old NMR electronics introduces a small disturbance to the signal at 11 and 70 ms, where it takes voltage signals for internal SFC calculation, as can be seen in Figs. 1 and 2. We therefore chose to sample the signal at 9.6 and 67.6 ms,

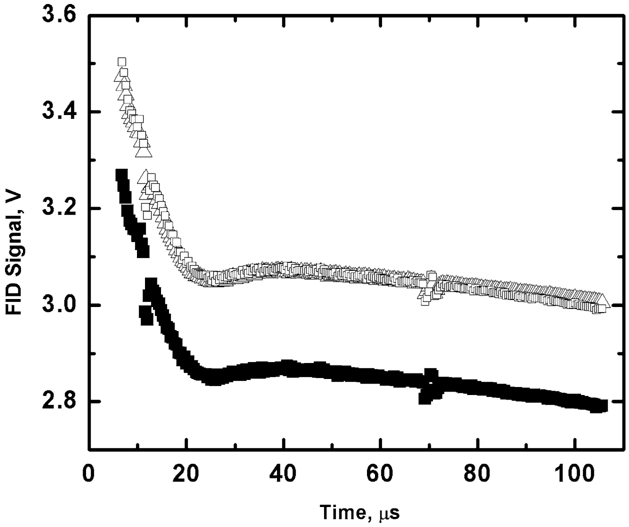

Fig. 1 Free induction decay (FID) signal in volts (*V*) as a function of time in microseconds (µs) for a sample of 20% canola stearin (CS) in canola oil stabilized inside the NMR magnet for 4 h without applied shear. The *open triangles* represent the signal obtained with a regular 10-mm NMR tube without the Teflon shaft. The *filled squares* represent the signal obtained for the same material stabilized inside the NMR magnet for 4 h but with the Teflon shaft inside the tube. The *open squares* represent the signal obtained from the tube with the shaft multiplied by a constant factor of 1.072. As can be seen the two signals superimpose almost exactly for the first 100 µs, indicating that we can obtain reliable SFC measurements with the Teflon shaft in place

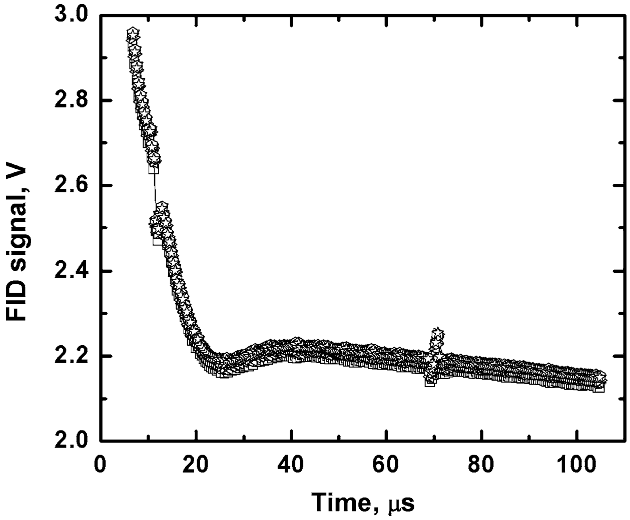

Fig. 2 Free induction decay (FID) signal in volts (*V*) as a function of time in microseconds (µs) for a sample of 40% canola stearin (CS) in canola oil stabilized inside the NMR magnet for 4 h, under a shear rate of 230 s^{-1}. Eight FID curves have been plotted together. They were obtained by alternating the motor on and off for periods of 10 min. Therefore, four FID curves were obtained under the applied shear whereas four were obtained without shear rate applied. As can be seen the eight signals superimpose almost exactly for the first 100 µs, indicating that we can obtain reliable SFC measurements with and without shear applied by the Teflon shaft. There is no significant difference either in the measured SFC, 26.1% with shear and 25.9% without shear

and calibrate our measurements from those values in a similar way as the instrument does.

The equation used by the Bruker instrument to calculate the relative ratio is

$$\mathrm{SFC} = \frac{[S - Lk]F}{[S - Lk]F + Lk} \times 100 \qquad (2)$$

where S is the solid signal measured at 11 µs and L is the signal measured at 70 µs (59 µs later). Since we sampled the signal at slightly different times, our values for k and F were different from those of the electronics of the NMR instrument. The factor k is the extrapolation factor for the liquid (1.0065) and F is the extrapolation factor for the solid (1.493). A digital offset was added to both S and L, which was determined by the NMR (0.094 V). The values were obtained from fitting our measurements from the FID of the calibration standards provided by Bruker (0, 31.9 and 74.3% SFC). It must be noted that the β and β' polymorphs often produce a different FID shape than the alpha polymorph, which decays similar to the standards. The signals from the β and β' polymorphs induce a deformation of the total signal, as described in the literature [12]. Fractionation may also affect the actual SFC values [14], since the relative density of protons in different fractions are not necessarily equal.

Direct Method of SFC Determination

SFC kinetics experiments were conducted by melting the sample in a beaker at 80 °C and then transferring it quickly to the NMR. Sample curves are presented in Fig. 3. The effect of shear is strongly observed in the 10% CS solution, and less obvious in the 40% CS solution. Note that although the solutions were prepared by weight, the solubility of CS in CO determines the actual final SFC. The lower SFC at higher shear rate is suspected to be due to the viscous heat generation produced by the shear energy. This is of importance in designing and calculating shearing devices that are intended to produce a particular final product.

A plot of the measurements taken after 2 h of equilibrating in the NMR using our own computer system are presented against the measurements reported by the instrument electronics in Fig. 4. It can be seen that there is a strong agreement between the values ($r^2 = 0.999$).

A very important advantage of the direct SFC method is that it is very insensitive to the temperature of the sample.

Indirect Method of SFC Determination and Temperature Estimates

The liquid signal is sensitive to the amount of liquid present and to the temperature of the liquid. With the intention of combining the direct and indirect methods to estimate possible viscous heating under shear flow, we used the slower data sampler connected to the computer to acquire the liquid signal. The curves were evaluated the same as in the direct method, where 10 signals were averaged, although these signals were fitted using Gaussian peak fit analysis to determine the maximum liquid signal, which would be used in the SFC calculation.

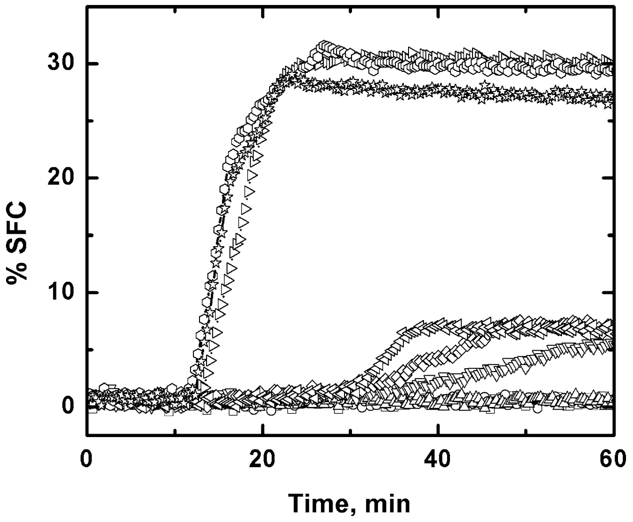

Fig. 3 Solid fat content (SFC) (%) of three different materials under different shear rates as a function of time in minutes. The time was recorded from the moment that the data acquisition system was turned on, after the molten sample had been introduced in the probe inside the magnet. The symbols that stay around 0% correspond to pure canola oil, that remained liquid at 40 °C. The *inverted triangles* correspond to a 10% CS in CO system, crystallized statically; the *diamonds* to the same system under a shear rate of 50 s^{-1}, and the *left pointing triangles* to this system under 200 s^{-1}. The *triangles pointing right* correspond to a 40% CS in CO system without shear, the *circles* for this system under 50 s^{-1}, and the *stars* for this system under 200 s^{-1}. The *curves* are the average of three replicates, which were very close to each other. See text for discussion

With this method, CS solutions of 0, 10, 20 and 40% were used at several shear rates ranging from 0 to 460 s^{-1}. The sample height was approximately 27 mm with the shear shaft in place. These samples were also brought to 80 °C for 5 min, and placed in the NMR for 4 h. The liquid signals were aligned in time and averaged to show the effect of crystallization under shear flow on the liquid signal, as presented in Fig. 5 for the first 60 minutes of the experiments. As noted in the direct method, the effect of shear on the kinetics of crystallization was very noticeable with the 10% CS solution, while there was less impact on the higher concentrations (20 and 40% CS).

Inside this NMR instrument, the temperature is kept at 40 °C. The tube containing the shaft, initially at 80 °C, takes about 40 min after being placed in the NMR to be stabilized at 40 °C. As shown in Fig. 5 (liquid CO lines), the liquid signal intensity increases as the liquid cools down. To estimate the temperature profiles of the cooling

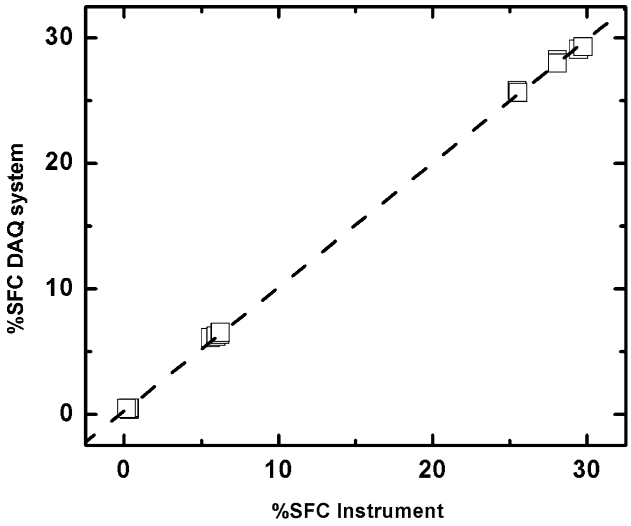

Fig. 4 Solid fat content (SFC) calculated by our data acquisition program (DAQ) vs. SFC calculated by the electronics of the NMR system, under different conditions of SFC and shear rates, after long time (2 h or more) of stabilization inside the NMR magnet. It can be seen that the correlation is excellent, proving that our data acquisition system provides reliable results compared to the standard electronics of the NMR machine

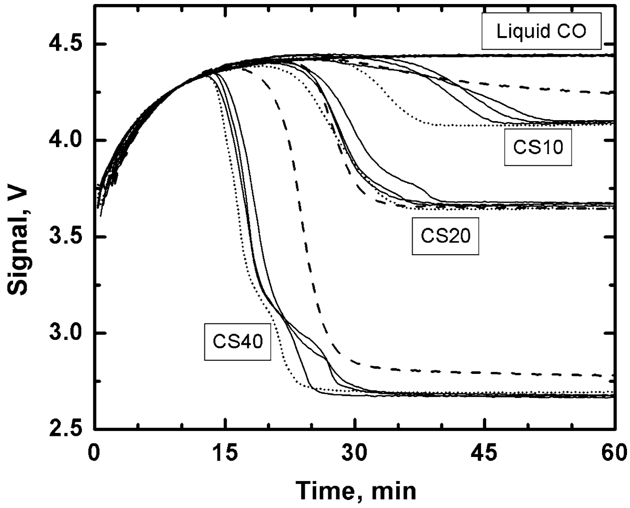

Fig. 5 Liquid signal (*V*) as a function of time (min) for experiments with different solutions of canola stearin (CS) in canola oil (CO), at different shear rates. Pure canola oil, 10% CS in CO (CS10), 20% CS in CO (CS20) and 40% CS in CO (CS40). The *dashed line* of each data set is for the static experiments (no shear flow) and the *dotted line* for the experiments at 460 s^{-1}. The shear rates in between are represented by thin solid lines

samples, plots of temperature versus time were created placing a thermistor inside an NMR tube and obtaining the ratio of the signal intensity at each temperature to the intensity of the liquid after equilibrating for 4 h at 40 °C. These signal ratios are plotted against temperature in Fig. 6. No significant difference was found between pure liquid canola oil and a saturated solution of canola stearin in canola oil, which would have been the liquid present in the determinations done for CS10, CS20 and CS40. The data were fitted to the parabola

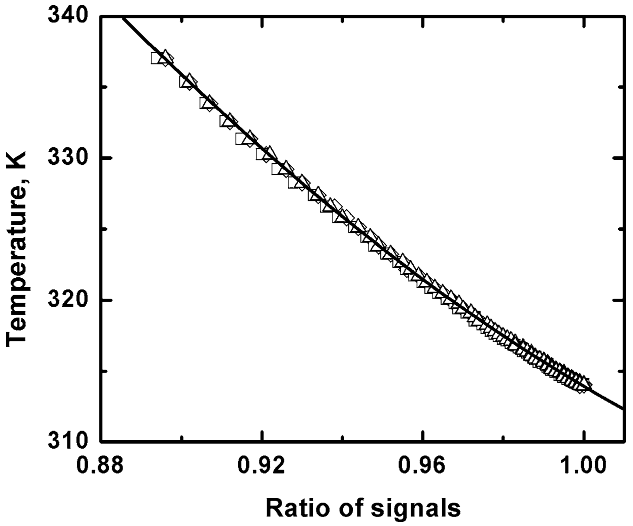

Fig. 6 Absolute temperature in K as a function of the ratio of intensity of the liquid signals. The ratio is computed between the liquid signal at the given temperature and the liquid signal at the equilibration temperature (ca. 40 °C). The *diamonds* represent pure canola oil, the *squares and triangles* the saturated solution of canola stearin in canola oil. Both materials fit the same parabolic Eq. 3 (*solid line*), as explained in the text

$$T = A + B_1 \cdot X + B_2 \cdot X^2 \tag{3}$$

where X is the ratio of signals, T is temperature in K, and $A = 993.5 \pm 9.9$, $B_1 = -1191 \pm 20.7$ and B_2 511.3 ± 10.8, with an $r^2 = 0.99978$. This equation was used to estimate the temperature of the liquid canola oil after placing it in the NMR magnet. The ratio between the signal at any given time and the signal after equilibration was used as X in Eq. 3, and the estimated temperature of the liquid was plotted in the right axis of Fig. 7 (circles). The estimated temperature data were fitted to a single exponential, as shown by the solid line. The excellent agreement suggests that the cooling process follows a lumped mode. This heat transfer mode is present at very slow external heat transfer conditions compared to the heat transfer inside the tube. This explains why the little amount of heat released by the cooling or even by the crystallization events of the small sample did not affect the temperature of the massive magnet. The magnet has a sensitive temperature sensor that displays an error if its temperature is off by more than about ±0.2 °C. The error condition was never triggered, meaning that the temperature of the magnet was not compromised. As time went by the temperature eventually equilibrated with the surroundings. Therefore after 4 h it is reasonable to expect that the heat of crystallization or the heat released by cooling would have been effectively dissipated.

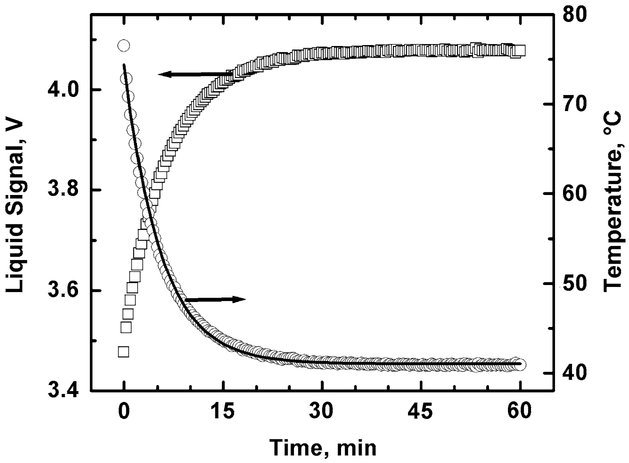

Fig. 7 Liquid signal in volts (*left axis, squares*) as a function of experimental time in minutes, recorded from the moment that the data acquisition program was started a few moments after introducing the hot NMR tube with the shaft into the NMR holder. The right axis presents the temperature (*circles*) calculated from the liquid signal using Eq. 3 and the fit to an exponential decay (*solid line*) characteristic of a lumped system cooling behaviour

The cooling pattern for pure canola oil statically or under a shear rate of 460 s^{-1} was the same, as seen in Fig. 5 (liquid CO lines). Therefore it seems that in this particular setup the shear flow has very little heat transfer enhancement effect, due very likely to the poor heat transfer conditions between the probe that holds the NMR tube and the 40 °C environment that surrounds it. Thus, when viscous heating was present, it was to expect that the temperature of the sample would have been kept at a steady higher temperature than the environment of the NMR magnet. However, the amount of heat released was too small to trigger the overtemperature error of the magnet. On the other hand, static samples that had been allowed to crystallize for long time would have reached thermal equilibrium and dissipated all the crystallization heat, thus reaching the temperature of the magnet.

The SFC was calculated from the difference in the liquid signal using the indirect method:

$$\mathrm{SFC} = \frac{(\mathrm{Lo}_{40} - \mathrm{Ls}_{40})}{\mathrm{Lo}_{40}} \times 100 \tag{4}$$

where Lo_{40} is the CO signal at 40 °C, Ls_{40} is the liquid signal of the sample (CS 10, 20 or 40) at 40 °C.

The tube was placed in the NMR for 4 h, to allow for thermal and crystallization equilibration. Then, the SFC computed only from the liquid signal using the indirect method was compared with the SFC output of the NMR display (direct method). The direct method determination averaged 10 signals per measurement, and 15 repetitions of each measurement were taken sequentially and averaged.

Using only the raw data, we found a large difference in the SFC values from the indirect method compared to the SFC from the direct method for statically crystallized samples. This inconsistency was produced by not taking into account two factors: the major one is the mass of material in the NMR detection volume, and the minor one is the small contraction due to the crystallization of the CS. The indirect method is very sensitive to the amount of material in the detection volume, since it measures the signal from the total amount of material, rather than the ratio between solid and liquid. To correct for imprecision in the measurement of the sample quantity, a calibration was performed by placing different amounts of liquid in the system and measuring the liquid signal after thermal equilibration, as seen in Fig. 8. Thus, for a given mass of sample it is possible to estimate the correct liquid signal Lo_{40} and calculate the SFC using Eq. 4. The mass correction can be avoided if the tube is filled above the detection volume of the NMR. The contraction correction would still be necessary. In our case we measured a contraction of about 3% for the CS40 sample. We assumed that the contraction for the CS20 was about half of that, and for CS10 about one quarter.

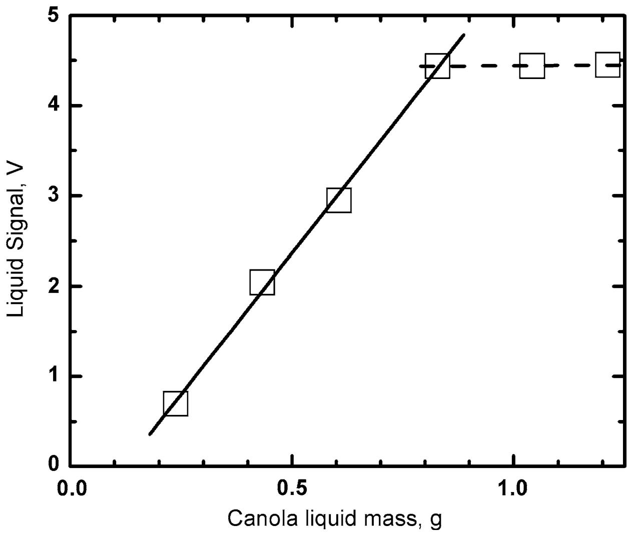

Fig. 8 The *squares* correspond to the signal from the liquid in the NMR in volts, versus mass of canola oil placed in the NMR tube with the shaft, in grammes. The *solid line* shows the linear fit to the points including the maximum detection mass and smaller values. The *dashed line* represents the linear fit to the values above the maximum detection mass

After applying both corrections to the data, we plotted the results as shown in Fig. 9. The values for the static experiments, and those for the low SFC correspond reasonably well to the actual SFC.

As the SFC and the shear rate are increased, the indirect SFC values appear higher than the actual SFC. This is due to an increase in temperature produced by viscous heating. This viscous heating is responsible for the reduction of the SFC at higher shear rates, compared to static experiments.

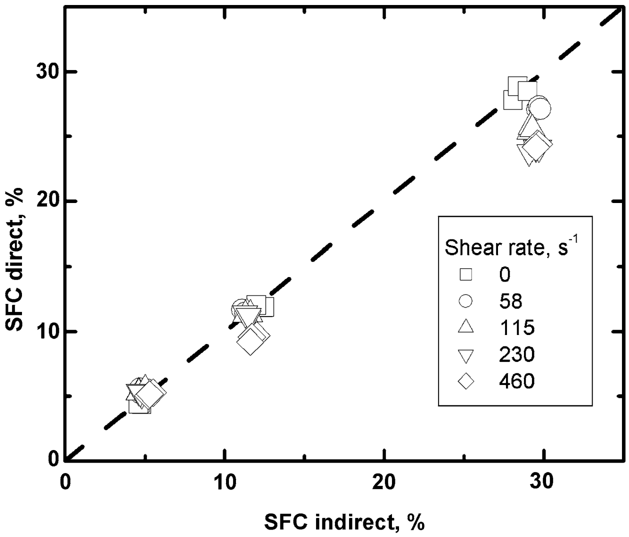

Fig. 9 SFC measured (direct method) after 4 h of equilibration for each one of the experiments presented in Fig. 5, as a function of the SFC calculated using the liquid signal (indirect method) and including corrections for mass of sample and sample contraction. The *dashed line* indicates the expected agreement. The *different symbols* correspond to the shear rates indicated in the figure

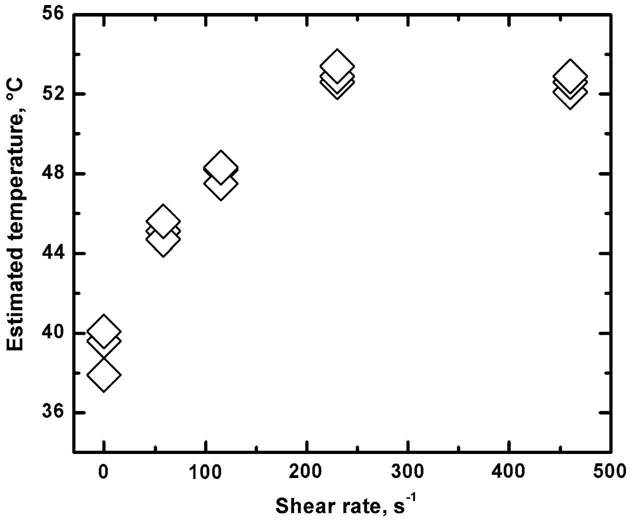

Fig. 10 Estimated temperature of the liquid, (°C), as a function of the shear rate applied for the CS40 sample crystallized for 4 h

At low SFC or low shear rates, the viscous heat generated is very small. However at the higher SFC and higher shear rates it becomes significant. The following procedure can be used to estimate the temperature resulting from the viscous heating: The expected signal $Ls_{40\text{-}E}$ can be calculated from Eq. 4 using the direct SFC and the Lo_{40} signal (corrected). Then we compute the ratio X between the actual signal obtained at temperature T and the liquid signal expected from the SFC, $X = Ls_T/Ls_{40\text{-}E}$. This ratio X can then be used in Eq. 3 to estimate the temperature of the liquid. The estimated temperatures for the CS40 sample are plotted in Fig. 10 as a function of the applied shear rate.

The power per unit volume delivered through mechanical agitation to a Newtonian fluid increases with the square of the shear rate. The figure shows a very different behaviour, since it tapers off at the higher shear rates. This can be explained by heat transfer conditions combined with the changes in apparent viscosity expected for this non-Newtonian system. The steady state temperature will be reached when the rate of delivery of mechanical energy to the system becomes equal to the rate of outbound heat transfer. Increasing the temperature increases the rate of outbound heat transfer until a steady state is reached.

On the other hand, in a non-Newtonian suspension the viscosity will decrease as the SFC is reduced, if other parameters are constant. Additionally, fats crystallized under shear tend to form platelets that orient parallel to the flow [7]. The degree of orientation increases with the shear rate [15], and this should result in further decrease of the viscosity. Shear also can modify the crystal size distribution, which also has an impact on the apparent viscosity. Thus, the final temperature at each shear rate depends on a large number of factors. The possibility of estimating the temperature from an intrinsic property of the liquid (the NMR signal) offers new and unique possibilities for the study of crystallization of lipids under shear flow.

Potential for this Method

The importance of this work is that it offers a possibility of closing a gap of knowledge in the development of kinetic models for crystallization under shear. As explained in the papers on crystallization of lipids under shear using synchrotron radiation, the ratio of solid phase to integrated intensity cannot be calculated a priori. This is in part due to the presence of mixed crystals and in part due to the complex geometries and systems that are needed to crystallize a sample under shear [9, 10]. Yet it is essential to obtain these quantitative relationships. Since shear flow affects the crystallization pathways and kinetics, only experiments measuring directly SFC under shear flow conditions can be compared to the experiments done using synchrotron radiation [10]. The method of temperature estimation is important because it is very difficult to place a temperature sensor in small shear cells without disturbing the shear flow or without exchanging heat with cell. Thus, this proof of concept finally opens the door to the possibility of developing substantially better quantitative models.

This apparatus can be applied to all lipid systems, provided a temperature control system for the sample is incorporated inside the magnet, as will be shown in a following paper. In the absence of internal temperature control, the shear can be applied keeping the sample under shear in the NMR tube in an external bath, or put through a specific tempering process according to a manufacturer's process, and then placed into the NMR magnet. The amount of heat transfer in the first few minutes is slow, and would have little effect on the sample. SFC can be determined according to the specific design of the process, or new processes can be developed in order to increase the desirable attributes of the fat product.

Understanding the effects of shear flow on the volume fractions of nanostructured lipid multicomponent systems is very important. It will permit, for instance, thoughtful tailoring of innovative edible products such as spreads and bakery shortenings made with zero-*trans* and low-saturated content and optimize their manufacturing processes.

Acknowledgments We acknowledge the financial support from the National Science and Engineering Research Council of Canada, and we are grateful for the loan of the Minispec from Dr. A. Marangoni, as well as to Naomi Hughes for preliminary exploratory experiments. The technical support and discussions from Dr. Peter Krygsman (Bruker) are gratefully acknowledged.

References

1. Mazzanti G, Guthrie SE, Marangoni AG, Idziak SHJ (2006) Synchrotron advances at the frontiers of food physics: studies of edible fats such as chocolate under shear Phys Can 62(5):313–320
2. Braipson-Danthine S, Deroanne C (2006) Determination of solid fat content (SFC) of binary fat blends and use of these data to predict SFC of selected ternary fat blends containing low-erucic rapeseed oil. J Am Oil Chem Soc 83(7):571–581
3. Ibanez E, Cifuentes A (2001) New analytical techniques in food science. Crit Rev Food Sci 41(6):413–450
4. Martini S, Bertoli C, Herrera ML, Neeson I, Marangoni A (2005) In situ monitoring of solid fat content by means of pulsed nuclear magnetic resonance spectrometry and ultrasonics. J Am Oil Chem Soc 82(5):305–312
5. Martini S, Herrera ML, Marangoni A (2005) New technologies to determine solid fat content on-line. J Am Oil Chem Soc 82(5):313–317
6. Torbica A, Jovanovic O, Pajin B (2006) The advantages of solid fat content determination in cocoa butter and cocoa butter equivalents by the Karlshamns method. Eur Food Res Technol 222(3–4):385–391
7. Mazzanti G, Guthrie SE, Sirota EB, Marangoni AG, Idziak SHJ (2003) Orientation and phase transitions of fat crystals under shear. Cryst Growth Des 3(5):721–725
8. Mazzanti G, Guthrie SE, Sirota EB, Marangoni AG, Idziak SHJ (2004) Novel shear-induced phases in cocoa butter. Cryst Growth Des 4(3):409–411
9. Mazzanti G, Marangoni AG, Idziak SHJ (2005) Modeling phase transitions during the crystallization of a multicomponent fat under shear. Phys Rev E 71(April):041607
10. Mazzanti G, Guthrie SE, Marangoni A, Idziak SHJ (2007) A conceptual model for shear-induced phase behavior in crystallizing cocoa butter. Cryst Growth Des 7(7):1230–1241
11. Callaghan PT (2006) Rheo-NMR and velocity imaging. Curr Opin Colloid Interface Sci 11:13–18
12. Van Duynhoven J, Dubourg I, Goudappel GJ, Roijers E (2002) Determination of MG and TG phase composition by time-domain NMR. J Am Oil Chem Soc 79(4):383–388
13. Van Putte K, Van Den Enden J (1974) Fully automated determination of solid fat content by pulsed NMR. J Am Oil Chem Soc 51:316–320
14. Marangoni AG, Wright AJ, Narine SS, Lencki RW (2000) Comment on the use of direct pulsed nuclear magnetic resonance solid fat content measurements in phase behavior studies of lipid mixtures. J Am Oil Chem Soc 77(5):565–567
15. Mazzanti G, Guthrie SE, Sirota EB, Marangoni AG, Idziak SHJ (2004) Crystallization of bulk fats under shear In: Dutcher JR, Marangoni AG (eds) Soft materials—structure and dynamics. Marcel Dekker, New York